IAEA
International Atomic Energy Agency

20th IAEA Fusion Energy Conference
Vilamoura, Portugal, 1-6 November 2004

IAEA-CN-116/TH_P4_35

Nonthermal Particle and Full-Wave Diffraction Effects on Heating and Current Drive in the ICRF and LHRF Regimes

J. C. Wright† 1), L. A. Berry 2), P. T. Bonoli 1), D. B. Batchelor 2), E. F. Jaeger 2), M. D. Carter 2), E. D'Azevedo 2), C. K. Phillips 3), H. Okuda 3) R. W. Harvey 4). D. N. Smithe 5), J. R. Myra 6), D. A. D'Ippolito 6), M. Brambilla 7), R. J. Dumont 8)

1) MIT Plasma Science and Fusion Center - Cambridge, MA, USA
2) Oak Ridge National Laboratory - Oak Ridge, TN, USA
3) Princeton Plasma Physics Laboratory - Princeton, New Jersey, USA
4) CompX Corporation - Del Mar, CA, USA
5) Mission Research Corp. - Newington, VA, USA
6) Lodestar – Boulder, CO, USA
7) Max-Planck-Institut für Plasmaphysik - Garching bei München, Germany
8) Association EURATOM-CEA sur la Fusion – Cadarache, France

† Primary author email: jwright@psfc.mit.edu

Nonthermal Particle and Full-Wave Diffraction Effects on Heating and Current Drive in the ICRF and LHRF Regimes

J. C. Wright† 1), L. A. Berry 2), P. T. Bonoli 1), D. B. Batchelor 2), E. F. Jaeger 2), M. D. Carter 2), E. D'Azevedo 2), C. K. Phillips 3), H. Okuda 3) R. W. Harvey 4). D. N. Smithe 5), J. R. Myra 6), D. A. D'Ippolito 6), M. Brambilla 7), R. J. Dumont 8)

1) MIT Plasma Science and Fusion Center - Cambridge, MA, USA
2) Oak Ridge National Laboratory - Oak Ridge, TN, USA
3) Princeton Plasma Physics Laboratory - Princeton, New Jersey, USA
4) CompX Corporation - Del Mar, CA, USA
5) Mission Research Corp. - Newington, VA, USA
6) Lodestar – Boulder, CO, USA
7) Max-Planck-Institut für Plasmaphysik - Garching bei München, Germany
8) Association EURATOM-CEA sur la Fusion – Cadarache, France

Abstract Fast waves (FW) are a primary technique for heating and current drive (CD) on the proposed burning plasma device, ITER, and lower hybrid (LH) waves are a candidate for edge current profile control. The models used to simulate these two waves rely on assumptions of Maxwellian populations that allow efficient analytic implementations of the plasma response, and in the case of the LH wave, the ray tracing models used are able to follow the very small wavelengths in a continuum manner without requiring a fine computational grid. Recent advances in algorithms and parallel computational methods have allowed these assumptions to be tested, permitting more accurate estimates of heating deposition and CD efficiencies in a burning plasma. Absorption by energetic particles for both waves can be significant, reducing electron heating and associated CD. Wave propagation and absorption is dependent on the velocity space distribution of particles in the plasma and on the geometric effects of focusing and diffraction. Fusion born alpha particles and neutral beam ions may interact with these waves in a manner that cannot be accurately modeled by Maxwellian distributions. The AORSA2D code has been modified to use a generalized non-Maxwellian conductivity, and has been applied to ITER reference scenarios. Preliminary analysis for ITER suggests that alpha absorption may be limited to a few tens of percent, and thus, allow reasonable CD efficiencies, assuming that the RF does not significantly alter the alpha slowing-down distribution. We also discuss the interaction of an energetic Tritium tail with FW in ITER. In addition, the effects of diffraction on LH waves in toroidal geometry are not well understood because computational limits have prohibited full-wave simulations at those small wavelengths. Simulations of LH waves have been restricted to WKB ray tracing techniques and 1D full-wave in the past, but the availability of massively parallel architectures have made full-wave calculations using an electromagnetic field solver tractable. The TORIC code has been adapted to run on parallel architectures making it possible to resolve the slow electrostatic LH wave. We present full-wave simulations of LH slow and fast waves in toroidal geometry for Alcator C-Mod at values of $(\omega_{pe}/\omega_{ce})^2$ comparable to those expected in the ITER device.

1. Introduction

Heating and current drive (CD) using radio frequency (RF) waves is an established technique in plasma fusion research. Fast waves (FW) in the ion cyclotron range of frequencies (ICRF) are to be used for both heating and non-inductive CD on the ITER device. Progress has also been made in reactor relevant performance of LH waves [1], and they have been proposed for ITER as a method of edge current profile control [2]. The models used to simulate these two waves have relied on assumptions of Maxwellian populations that allow efficient analytic implementations of the plasma response.

Absorption by energetic neutral beam fast ions, alpha particles, or from RF-driven minority tails can be significant and reduce electron heating and associated current drive. In the case of the LH wave, the WKB ray tracing models used are able to follow the very small wavelengths in a continuum manner without requiring a fine computational grid, but this technique ignores diffraction and focusing [3]. Recent advances in algorithms and parallel computation have removed these assumptions and lead to more accurate estimates of heating deposition and CD

† Primary author email: jwright@psfc.mit.edu

efficiencies in a burning plasma.

$$\nabla\times\nabla\times\mathbf{E} = \frac{\omega^2}{c^2}\left\{\mathbf{E} + \frac{4\pi i}{\omega}\left(\mathbf{J}^P + \mathbf{J}^A\right)\right\} \leftarrow \mathbf{E}(\mathbf{x}) = \sum_m \mathbf{E}_m(\psi)\exp\left(im\theta + in\phi\right) \qquad (1)$$

Quantitative analysis of these phenomena require 2D full-wave electromagnetic modelling with finite Larmor radius interactions for non-Maxwellian distribution functions. This involves solving the system described in Equation (1) with varying choices of decomposition for the electric field, **E**, and of the plasma response in $\mathbf{J}_p$. For initial assessments, we use either model distribution functions based on collisional slowing down processes or distributions calculated by the CQL3D [4] Fokker-Planck model that also includes the effects of RF-driven diffusion, but with approximate quasilinear terms. However, in the longer term, self-consistent particle distribution functions that are iterated with the RF calculations are necessary. Full-wave studies of LH waves have been done in one dimension [5], but the computational requirements for two dimensional (2D) simulations have been prohibitive. Accurate 2D models are needed to capture the effects of geometric focusing, wave interference, and diffraction effects. In this paper, we present calculations of LH slow and fast wave propagation in Alcator C-Mod and of alpha particle absorption of FW in ITER in 2D toroidal geometry.

The RF modelling of the FW absorption on alphas and neutral beams uses the All-Orders Spectral Algorithm (AORSA) full-wave code [6] in combination with self-consistent particle distributions from the CQL3D Fokker-Planck code [4]. Aggressive parallelization and vectorization, the development of more efficient algorithms for the evaluation of the plasma dielectric for non-Maxwellians, and the use of very large scale parallel architectures has permitted the coupling of these two codes. AORSA has been extended to include modifications of the plasma conductivity due to non-Maxwellian distribution functions [7]. For example, in ITER, we find the power absorbed by the alphas varies from 2% for a Maxwellian to 5% for the slowing down distribution. In contrast to the non-Maxwellian case, the Maxwellian model has very little power deposited in the plasma center. Preliminary analysis of the FW alpha damping using isotropic slowing-down distributions suggests that absorption may be limited to a few tens of percent allowing reasonable current drive efficiencies, assuming that the RF does not significantly alter the slowing-down distribution.

We have used the full-wave finite Larmor radius ICRF code, TORIC [8], for the LH analysis. By adapting the code to run on parallel architectures, its resolution limits were increased sufficiently to resolve mode converted ion Bernstein (IBW) and ion cyclotron (ICW) waves in Alcator C-Mod and Asdex Upgrade [9] as well as the slow electrostatic LH wave. We have modified the dielectric model in TORIC to describe waves in the LHRF accurately. The original ICRF antenna model in TORIC is used to simulated the launch of an inaccessible fast wave mode in the LHRF that converts to a slow wave and reflects from an edge cutoff. Using this model, we show full-wave effects on LH wave dynamics in tokamak plasmas. Differences in the power deposition profiles and upshift of the parallel wavenumber between the full-wave studies and ray tracing results and their applicability to the spectral gap problem will be discussed.

2. DESCRIPTION OF CLOSED LOOP ICRF COMPUTATIONS

An important problem in radio frequency (RF) heating of fusion plasmas is the absorption of power by non-Maxwellian components such as minority ion species, fusion-born alpha particles, and fast ions associated with neutral beam injection (NBI). Heating of these components can occur at high harmonics of the ion cyclotron frequency where conventional 2D full-wave models for RF heating are not valid. In this work, the 2D, all-orders full-wave model AORSA [6] is extended to include non-Maxwellian velocity distribution functions. Results show that the non-Maxwellian nature of the velocity distribution function affects wave propagation as well as power absorption.

To compute self-consistent wave fields and particle distribution functions, four different physics models must be integrated: (1) plasma conductivity for non-Maxwellian distribution functions; (2) a wave solver incorporating the non-Maxwellian conductivity; (3) the quasilinear (QL) operator [10] that drives non-thermal distributions (at present, we are using a approximate QL operator based on geometrical optics); and (4) a Fokker-Planck solver. In the near future, the loop will be closed by using a QL operator derived directly from the full-wave solution as described below. The long term goal is to develop an integrated wave simulation consisting of these four basic elements, all communicating and interacting in an automated way on the same computing platform.

Following Stix [11], we write the generalized plasma conductivity tensor for an arbitrary non-relativistic species. For non-Maxwellian distributions, the standard plasma dispersion function is replaced by 2D velocity space integrals for every mode in the wave spectrum at each point in space. These integrals have been programmed into a suite of subroutines referred to as the SIGMAD module [7][12][13]. To reduce the required computation time, the integrals have been vectorized, parallelized, and multi streamed.

In many cases of interest, the energy absorbed by the plasma, $\partial W/\partial t$, can be approximated by $1/2\ Re(\mathbf{E}^*\bullet\mathbf{J}_p)$ where $\mathbf{J}_p$ is the plasma current as calculated from the conductivity. However, when there is significant wave energy carried by thermal motion of the particles (i.e. kinetic flux), a more general expression is required [14]. This expression is quadratic in the electric field, and can be written in terms of nested sums over the two wave numbers, $\mathbf{k}_1$ and $\mathbf{k}_2$, associated with the two electric field vectors. When $\mathbf{k}_1 = \mathbf{k}_2$, the sums over $\mathbf{k}_1$ and $\mathbf{k}_2$ separate to give $\partial W/\partial t = 1/2\ Re(\mathbf{E}^*\bullet\mathbf{J}_p)$. When $\mathbf{k}_1 \neq \mathbf{k}_2$, five nested do loops are required in 2D, and seven in 3D, and calculating these sums can take orders of magnitude more computation than the wave solution itself. By bringing the velocity space integrals outside of the sums over $\mathbf{k}_1$ and $\mathbf{k}_2$, the sums can be separated, even for $\mathbf{k}_1 \neq \mathbf{k}_2$. This requires that the parallel velocity integral be done numerically rather than analytically. However, because the sums over $\mathbf{k}_1$ and $\mathbf{k}_2$ are separated, there is an enormous savings in computation time, and $\partial W/\partial t$ can be calculated in approximately the same time as the plasma current $\mathbf{J}_p$.

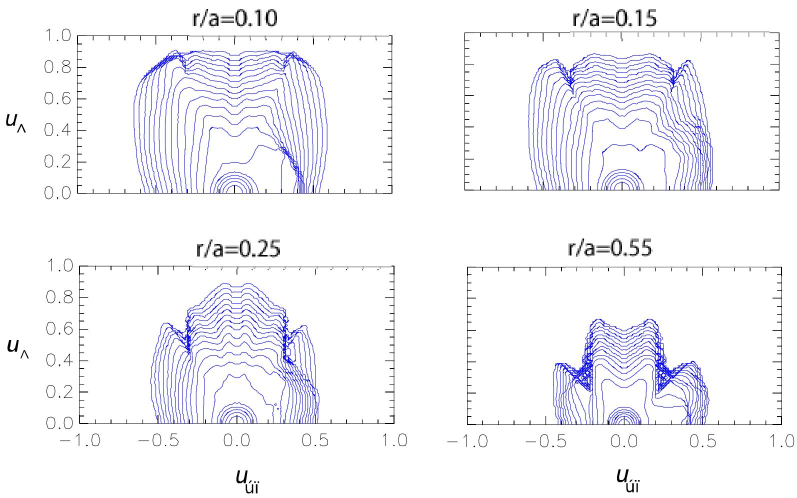

FIG. I: The ion distribution function for a neutral beam injection plasma with high harmonic fast wave heating in NSTX [15] shot #108251 calculated with the CQL3D code [4].

To solve the Fokker-Planck equation self-consistently with the full wave RF solution, the quasilinear diffusion coefficients must be derived directly from the full-wave RF electric field solution. These coefficients are closely related to the RF heating rate $\partial W/\partial t$ and can be found by writing $\partial W/\partial t$ in terms of the time derivative of the distribution function. Equating this expression to the plasma heating rate derived above, we can deduce expressions for the quasilinear diffusion coefficients

Figure I shows the ion distribution function for a neutral beam injection plasma with high harmonic fast-wave heating in NSTX [15] shot #108251 calculated with the CQL3D Fokker-Planck code [4]. The non-Maxwellian distribution function is shown at four different radial locations in the plasma. Figure II shows the power absorbed in NSTX calculated from AORSA[1]

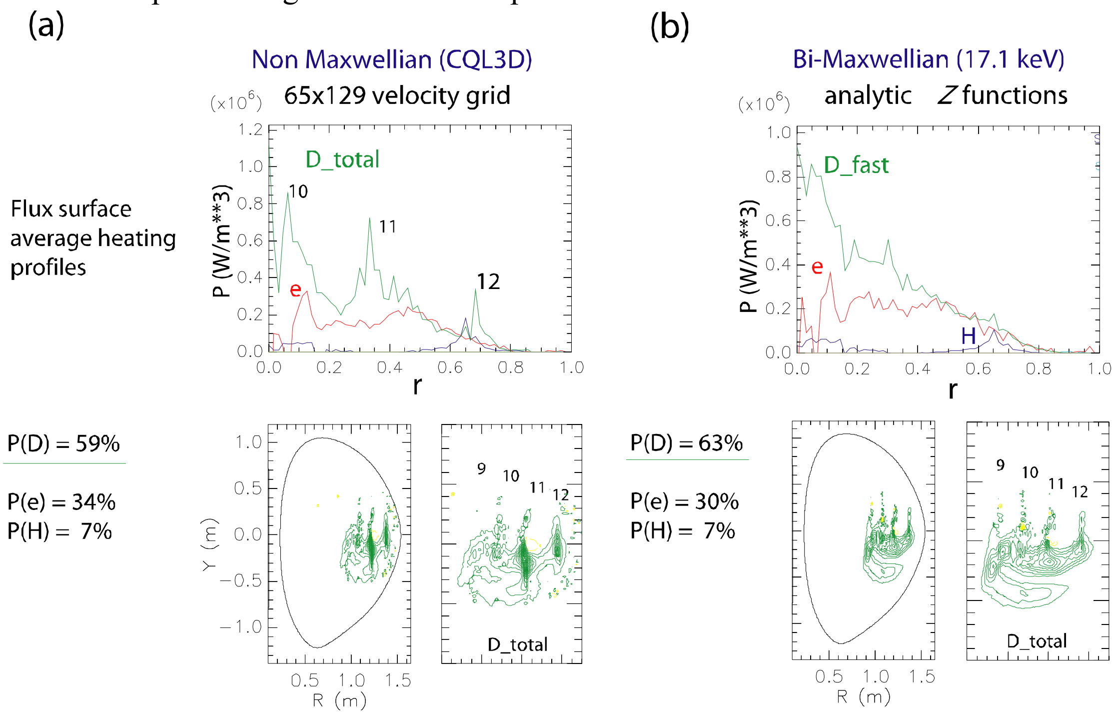

FIG. II: Power absorbed by neutral beam injection ions in NSTX (green) calculated (a) from the complete non-Maxwellian distribution in Fig. I and (b) from a bi-Maxwellian approximation.

using (a) the complete non-Maxwellian distribution in FIG. I and (b) a bi-Maxwellian approximation. Flux surface average heating profiles are shown for the non-Maxwellian neutral beam ions (green) and the Maxwellian electrons (red). Note that the power absorbed by the non-Maxwellian ions is highly localized near the 10th, 11th, and 12th harmonic resonances, and accounts for 59% of the absorbed power. The equivalent bi-Maxwellian model in FIG. II(b) gives approximately the same fractions of power absorbed, but the radial profile for the fast deuterium (green) is much more uniform. This is because the bi-Maxwellian distribution contains particles that extend to much higher energies than the non-Maxwellian, and therefore gives more Doppler broadening of the resonances. This broadening is clearly evident in the 2D contour plots in FIG. III(b) where the high harmonic resonances overlap in the lower half plane.

Another important example of a non-Maxwellian plasma component is the fusion-born alpha population in the proposed ITER [16] international burning plasma experiment. Figure III shows the power absorbed by these alpha particles as calculated from (a) the complete non-Maxwellian slowing down distribution function and (b) an analytic approximation that includes only dissipation and neglects the effect of the alpha particles on wave propagation. Flux surface average heating profiles are shown for the electrons (red) and tritium ions (blue), both assumed to be Maxwellian, and for the non-Maxwellian alpha particles (green). For the assumed frequency of 56 MHz, the power absorbed by the alphas is localized near the Doppler broadened first and second harmonic resonances, located just outside the plasma on the high and low field sides. In the non-Maxwellian case, the alphas account for 5% of the absorbed power. The approximate analytic model underestimates this fraction at 2%, with very little absorption near the center of the plasma. This difference occurs because the analytic model includes only the effect of energy dissipation and ignores the effect that the alpha particles have on wave propagation.

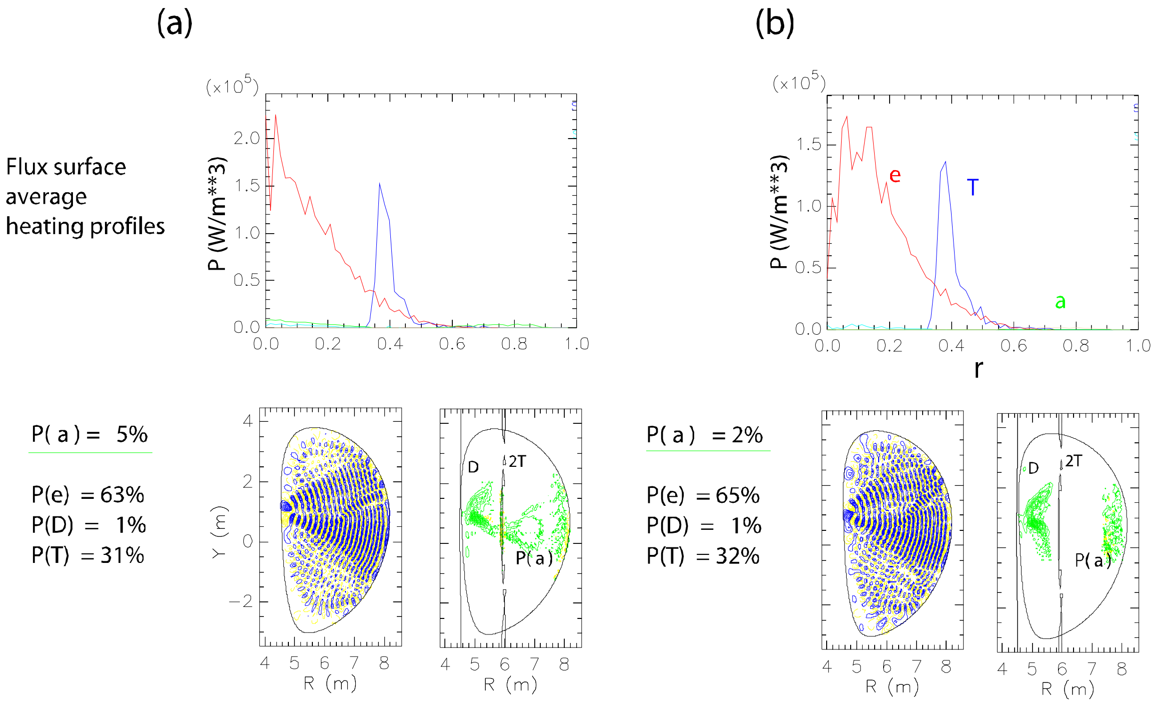

FIG. III: Power absorbed by fusion-born alpha particles in ITER (green) calculated (a) from the complete non-Maxwellian slowing down distribution and (b) from an analytic approximation.

3. Full-wave LHRF Studies

In the LH frequency range, the plasma contribution and the vacuum response embodied in the terms, $\mathbf{J}^p$ and $\mathbf{E}$, on the right hand side (RHS) of Equation (1) simplifies to the cold plasma contributions:

$$S\mathbf{E}_\perp + iD(\mathbf{b}\times\mathbf{E}_\perp) + P\mathbf{E}_\phi\mathbf{b}, \tag{2}$$

where S, D, and P, are the Stix cold plasma dielectric elements in the LHRF [11]. We may neglect the FLR terms which support the "pressure-driven" LH or ion plasma wave – it does not play any role in situations of interest and its wavelength is far too short to be resolved numerically, particularly in the plasma periphery. Also, the term does not change the dispersion of the remaining fast and slow LH waves. This system is in principle compatible with the TORIC discretization using cubic finite elements (FE). From the numerical point of view the wave equations, Equations (1) and (2), have only two independent solutions, and the FE discretization is spectrally polluted, independently of whether the FLR term is taken into account or not. Spectral pollution arises because Eqn. (2) contains no ψ-derivative of the E_ψ component (or, if FLR effects are retained, the coefficient of $dE_\psi/d\psi$ is far too small). As a consequence, the "exact" stiffness matrix would be singular or almost singular. Since the

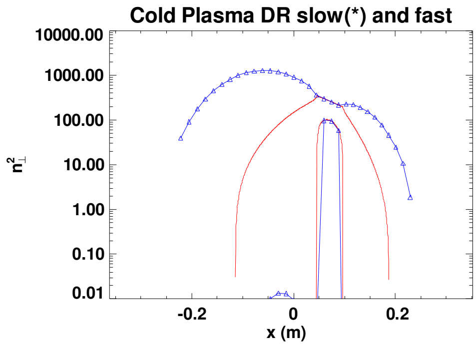

FIG. IV: Cold plasma electromagnetic dispersion relation for slow and fast LH waves using Alcator C-Mod parameters: [deuterium gas, $n_{\|}$=1.5, f_0 = 4.6 GHz, B_0 = 5.3T, T_e=3.5 keV, T_i=2.0 keV, I=1 MA, $n_e(0)$ =1.5 ×10^{20} m^{-3}.]

discretization is not "exact", the stiffness matrix can nevertheless be inverted, but the numerical solution turns out to be plagued by spurious oscillations on the mesh scale. This numerical instability has a simple physical explanation. Cubic finite elements guarantee the continuity of the electric field and its derivative (and hence of the wave magnetic field) at each point of the mesh. They are, therefore, ideal for the solution of 6th-order wave equations, with three independent eigenwaves (e.g. the two cold plasma waves and the pressure-driven wave). If the wave equations are of 4th order only, and thus possess only two independent modes, the discretization itself re-introduces the missing mode, with a wavelength dictated by the mesh step. Accordingly, this instability is known as "spectral pollution" and it corrupts the solution. In the simulations for this paper, to overcome the pollution problem and maintain numerical stability, the coefficient of the FLR term was increased to a finite value, but kept small enough to avoid affecting the wave dispersion. In addition, the LH TORIC algorithm now has boundary conditions appropriate for a waveguide - permitting coupling to both parallel and perpendicular components of the electric field to drive both the fast and slow lower hybrid waves.

We have used the TORIC solver to simulate LH slow and fast waves in toroidal geometry. Boundary conditions appropriate for a fast wave launch were used in the code and the sixth order wave equation was solved, which included the fast electromagnetic mode, the slow electrostatic wave, and the thermal ion plasma wave branch. In these studies the ion plasma wave was strongly evanescent, since ω/ω_{LH} >2. Coupling to the slow electrostatic wave was achieved by choosing plasma parameters so that the fast wave was inaccessible to the plasma center and mode converted to a slow wave at the confluence point between the two modes. This process is described by the cold plasma, electromagnetic dispersion relation plotted in FIG. IV. We have taken parameters typical of the upcoming LH current drive experiments on Alcator C-Mod [deuterium gas, $n_{\|}$=1.5, f_0 = 4.6 GHz, B_0 = 5.3 T, T_e=3.5 keV, T_i=2.0 keV, I=1 MA, $n_e(0)$ =1.5×10^{20} m^{-3}]. The fast wave (shown in red) starts propagating at its cutoff near x = 0.19m, and mode converts to a slow wave at the confluence point (x=0.08m). The slow wave then propagates out to its cutoff, undergoes a specular reflection at that point, and propagates back into the plasma.

This case was simulated with TORIC using 960 radial elements, 1023 poloidal modes, and required 2500 CPU hours utilizing 48 nodes on the MIT Beowulf cluster. The resulting electric field contours for $|Re(E_+)|$ are shown in FIGs. V. These contours clearly define a ring of accessible fast and slow LH waves propagating between the confluence point where mode conversion takes place and the cutoffs, where specular reflection occurs. A blow-up of this annular region is shown in the right panel of FIG. V. Remarkably, the electric field exhibits paths or filaments, extending from the edge cutoffs to the confluence that are reminiscent of the trajectories that would be formed in ray tracing for this type of case. Furthermore, the filaments tend to focus down to a narrow beam or caustic at the confluences.

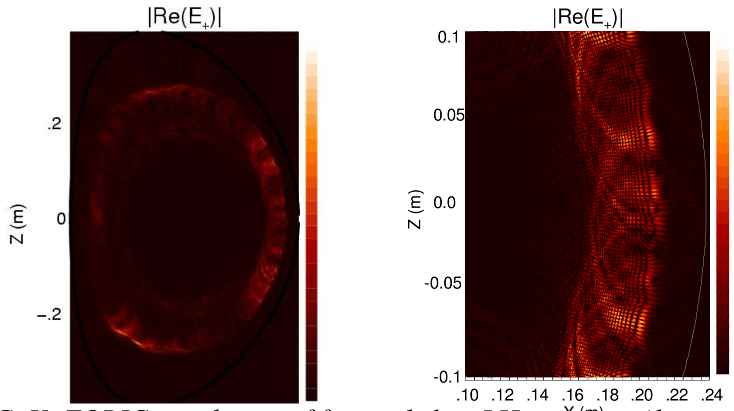

FIG. V: TORIC simulation of fast and slow LH waves in Alcator C-Mod. Right panel is an enlargement of low field side. [deuterium gas, $n_{\|}$=1.5, f_0 = 4.6 GHz, B_0 = 5.3T, T_e=3.5 keV, T_i=2.0 keV, I=1 MA, $n_e(0)$=1.5 $\times 10^{20}$ m^{-3}.]

The transverse dimension of the caustics formed in FIG. V can be comparable to the wavelength of the slow wave, in this case about 0.005 m. Significant spectral broadening due to diffraction can occur at these caustics [3]. This effect is not predicted within the geometrical optics framework. The spectral broadening can be seen by plotting the $|FFT\{Re(E_+)\}|$ versus the average parallel refractive index ($\langle n_{\|}\rangle$) on several flux surfaces, as shown in FIG. VI. The distribution of electric field amplitude on flux surfaces shows a significant upshift in the average launch $\langle n_{\|}\rangle$ of 2.0 to greater than 4.0 at r/a = 0.75, near the caustic surface. This increase in $n_{\|}$ is enough to cause the slow wave to damp via electron Landau damping at that location. The wave power is completely absorbed in this case in a layer between r/a of 0.68 to 0.80. We have also performed LH ray tracing calculations for the plasma parameters used in FIGs. V and VI. The ray trajectories exhibit multiple radial reflections similar to the field patters in FIG. V. No RF power is absorbed however, because the $n_{\|}$ variation is limited to $1.5 < n_{\|} < 2.5$ in the peripheral region where the wave is accessible. Eventually, after several radial reflections, the wave $k_{\|}$ is upshifted enough to allow propagation of the ray to the core, where it damps on electrons at $0.2 < r/a < 0.6$. The spectral broadening that occurs at the caustic within the full-wave framework is not included within the geometrical optics treatment and thus leads to fundamentally different absorption behavior.

This broadening due to diffraction could likely provide a ubiquitous mechanism by which LH waves are able to damp efficiently on electrons at $v_{\|} / v_{te}$ = 2-3, despite the fact they are injected at suprathermal speeds of (5-15) v_{te}.

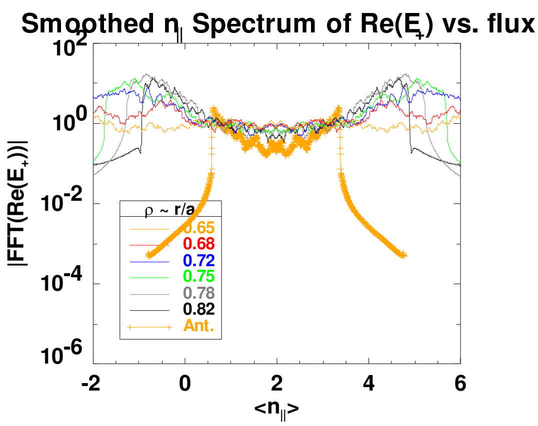

FIG. VI: $|FFT$ of $Re\{E_+\}|$ versus average $n_{\|}$ on several flux surface for the TORIC simulation of FIG. V. The $n_{\|}$ range shown corresponds to poloidal mode numbers in the range –511<m<+511.

4. Conclusions

Recent advances in algorithms and parallel computation have made it possible to carry out quantitative analysis of wave–particle interactions involving finite Larmor radius effects and non-Maxwellian distribution functions. The local RF conductivity operator has been evaluated in terms of arbitrary particle distributions using a new suite of modules SIGMAD. This general conductivity operator was then implemented in the all orders full-wave solver AORSA-2D. Using this combined model we have evaluated the parasitic effects of alpha particle damping for ICRF heating in the proposed ITER device and found the effect to be negligible (less than 5% of the total ICRF power). The non-thermal alphas were modeled with a slowing down distribution in this analysis. Parasitic damping of high harmonic fast waves on fast neutral beam ions in NSTX was also studied with the combined AORSA – SIGMAD model. Significant differences were found in the spatial distribution and magnitude of the parasitic absorption compared to calculations done with an energetic bi-Maxwellian for the beam ions.

Implementation of the TORIC full-wave solver on a massively parallel platform has made it possible to resolve both fast and slow LH waves in toroidal geometry for the first time ever. Full-wave analysis of LH waves in the Alcator C-Mod tokamak revealed the formation of caustic surfaces where the usual geometrical optics formulation is not valid. Analysis of the spectral distribution of electric field strength near these caustics showed significant broadening of the incident $n_{||}$ spectrum, presumably due to diffraction effects. The resulting increase in the parallel wavenumber spectrum may provide a well-defined mechanism by which LH waves are able to damp efficiently at (2-3)v_{te}, despite having been injected at phase speeds of (5-10)v_{te}.

5. Acknowledgments

This work was supported by a funding initiative from the U.S. Department of Energy titled Scientfic Discovery through Advanced Computing.

Bibliography

[1] G. BARBATO, "Recent progress in lower hybrid current drive theory and experiments", Plasma Phys. Controlled Fusion **40** (1998) A63.

[2] ITER Physics Expert Group on Energetic Particles, Heating and Current Drive, "Chapter 6: Plasma auxiliary heating and current drive", Nucl. Fusion **39** (1999) 2495-2540.

[3] G. V. PEREVERZEV, "Use of the Multidimensional WKB Method to Describe Propagation of Lower Hybrid Waves in Tokamak Plasmas", Nucl. Fusion **32** (1992) 1091-1107.

[4] R. W. HARVEY and M. G. MCCOY, "The CQL3D Fokker-Planck Code", IAEA (Madrid, 1992), Proc. of the IAEA Tech. Committee Meeting, Vienna (1993) 489-526.

[5] Y. PEYSSON, E. S'EBELIN, X. LITAUDON, D. MOREAU and J.-C. MIELL, "Full wave modelling of lower hybrid current drive in tokamaks", Nucl. Fusion **38** (1998) 939-943.

[6] E. F. JAEGER, L. A. BERRY, D. B. BATCHELOR and M. D. CARTER, "All-orders spectral calculation of radio-frequency heating in two-dimensional toroidal plasmas", Phys. Plasmas **8** (2001) 1573-1593.

[7] R. J. DUMONT, C. K. PHILLIPS, and D. N. SMITHE, "Effects of Non-Maxwellian Plasma Species on ICRF Propagation and Absorption", AIP (NY, 2003), Proceedings of the 15th RF Topic Conference, Moran (2003) 439.

[8] M. BRAMBILLA, "Numerical simulation of ion cyclotron waves in tokamak plasmas", Plasma Phys. Controlled Fusion **41** (1999) 1-34.

[9] J. C. WRIGHT, P. T. BONOLI, M. BRAMBILLA, F. MEO, E. D'AZEVEDO, D. B. BATCHELOR, E. F. JAEGER, L. A. BERRY, C. K. PHILLIPS and A. PLETZER, "Calculations of fast wave mode conversion and lower hybrid propagation in tokamaks", Phys. Plasmas **11** (2004) .

[10] C. F. KENNEL and F. ENGLEMANN, "Velocity Space Diffusion from Weak Plasma

Turbulence in a Magnetic Field", Phys. Fluids **9** (1966) 2377.

[11] T. H. STIX, The Theory of Plasma Waves, (1992).

[12] R. J. DUMONT, C. K. PHILLIPS, and D. N. SMITHE, "Effects of non-Maxwellian Species on Electromagnetic Wave Propagation and Absorption in Magnetically Confined Plasmas", Submitted to Phys. Lett. (2004) .

[13] R. J. DUMONT, C. K. PHILLIPS, and D. N. SMITHE, "ICRF wave propagation and absorption in plasmas with non-thermal populations", EPS (Geneva, 2002), Controlled Fusion and Plasma Physics, 26B, Montreaux (2002) paper P-5.051.

[14] D. N. SMITHE, "Local Full-Wave Energy and Quasilinear Analysis in Nonuniform Plasmas", Plasma Phys. Controlled Fusion **31** (1989) 1105.

[15] A. L. ROSENBERG, J. E. MENARD, J. R. WILSON, et al., "Fast ion absorption of the high harmonic fast wave in the National Spherical Torus Experiment", Phys. Plasmas **11** (2004) 2441.

[16] ITER Physics Expert Group, "Chap. 2: ITER Physics Basis: Plasma Confinement and Transport", Nucl. Fusion **39** (1999) 2175.